Complementing AGATA with MINIBALL

※

C. Domingo-Pardo[a], E. Farnea[b], A. Gadea[a], M. Labiche[c], J. Nyberg[d]

[a]IFIC, CSIC-University of Valencia, Valencia, Spain

[b]Istituto Nazionale di Fisica Nucleare, Sezione di Padova, Italy

[c]STFC Daresbury Laboratory, United Kingdom

[d]Uppsala University, Sweden

December 19, 2012

Abstract

This report summarizes the results of MC simulations, where a reference AGATA geometry of 5 double and 5 triple cluster detectors (5 ADC+5 ATC) is complemented with MINIBALL detectors. In all cases the common GSI beam conditions for in-flight γ-ray spectroscopy experiments have been included. This concerns projectile velocities of 100-150 MeV/u and the characteristic spatial beam profile at the final focal plane of GSI-FRS. Several possibilities have been considered for the MINIBALL geometry, always assuming that these detectors are mounted in the standard HECTOR holding structure. Thus, we find that by arranging 4 MTC at 95° and 4 MTC at 130° at a radial distance from the target of 25 cm, one can achieve an increase in photo-peak efficiency of more than 30%, with respect to the situation where only 5 ADC+5 ATC detectors are used. The energy resolution seems to be dominated, for both AGATA and MINIBALL, by effects due to *i*) energy loss of the projectile in the target (β-uncertainty) and *ii*) (for long halflives) the uncertainty at de-exciation z-position. Therefore, the lower position resolution of MINIBALL does not represent a major drawback in terms of γ-ray detection sensitivity. The latter is demonstrated by specific MC calculations which include target- and lifetime-effects in a realistic way.

1 General remarks

Unless otherwise stated, primary events are generated according to the spatial beam profile of GSI-FRS, which means 6 cm FWHM_x and 4 cm FWHM_y. The angular distribution for the emission of γ-rays from the secondary sample corresponds to a Lorentz boosted (at rest isotropic) distribution for $\beta = 0.43$ (∼100 MeV/u). The MC simulations reported in this work have been carried out with the Geant4 code described in Refs. [**?**, **?**] and more details about can be found therein.

2 Complementing 5 Double and 5 Triple AGATA Clusters with 5 MINIBALL Triple Cluster detectors

2.1 5 MINIBALL Triple Cluster detectors at 30 cm and forward angles

MINIBALL detectors are implemented in the simulation as triple clusters made from EUROBALL capsules. In these simulations, the MINIBALL detectors are always at a radius of 300 mm, being this radius 235 mm for the AGATA detectors. The following two configurations comprise always an inner ring of 5 AGATA Double Cluster detectors. The outer ring is made in the 5ADC+5ATC+5MTC configuration (Fig. 16) with 5 ATC packed together on the upper half and 5 Miniball Triple Cluster (MTC) covering the bottom half of the array. In the 5ADC+5(ATC+MTC) configuration (Fig. 2) the outer ring is made from semiconsecutive ATC and MTC detectors.

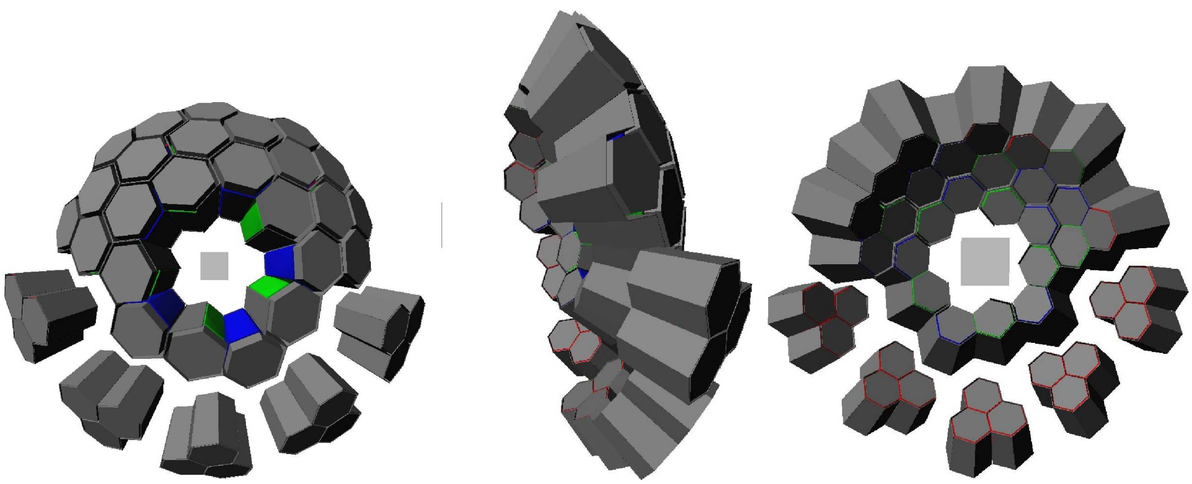

Figure 1: 5ADC+5ATC+5MTC Configuration, with MINIBALL at a radius of 300 mm (see report by J. Simpson)

The efficiency and P/T results of the latter two configurations are displayed in Fig. 2. These results were obtained with MGT. For sake of comparison, the results (without MINIBALL detectors) for the 5 ADC+10 ATC and 5 ADC + 5 ATC configurations are also shown.

Numerical values of the previous representations are tabulated in table 5. Differences versus the previous results reported at the MINIBALL Workshop are due to the larger radius (r = 300 mm) for the present simulation of MTCs.

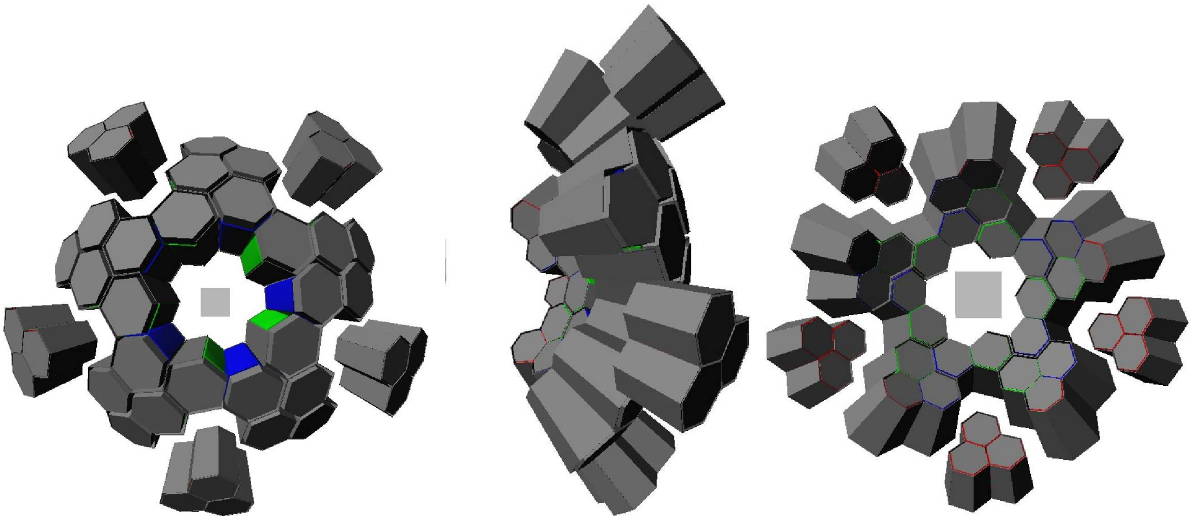

Figure 2: 5ADC+5(ATC+MTC) Configuration, with MINIBALL at a radius of 300 mm (see report by J. Simpson)

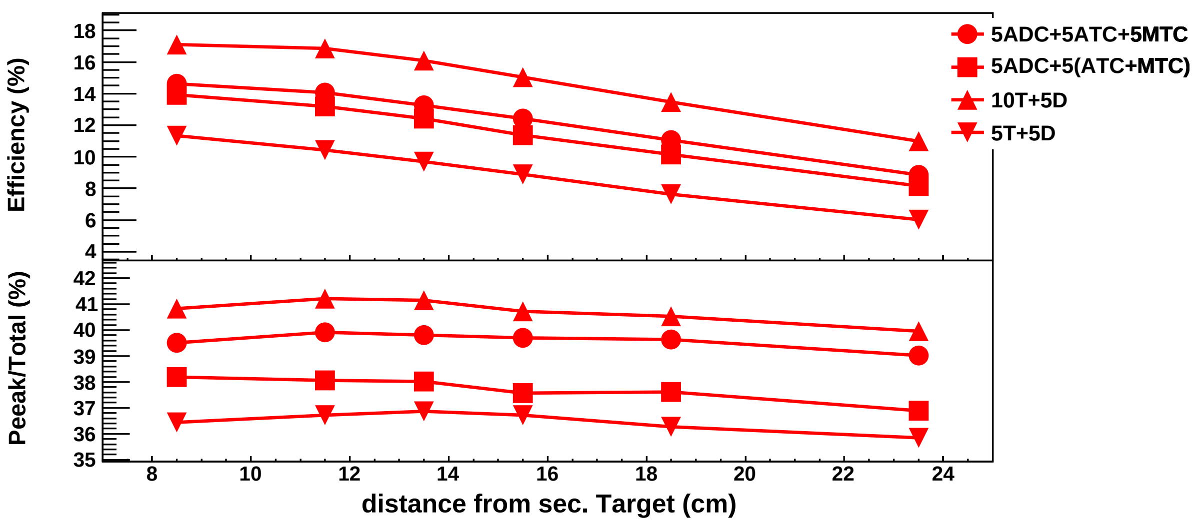

Figure 3: Efficiency for AGATA 5 D+5 T complemented with five Miniball triple cluster detectors at a radius of 300 mm (see legend and precious figures for geometry descriptions). Simulations for $\beta = 0.43$ and $E_{\gamma,\circ} = 1$ MeV.

Table 1: Performance of AGATA complemented with MINIBALL. See previous figures for a description of the setup. For each configuration indicated in the first column of the table, the two rows represent the efficiency and P/T ratio, respectively.

SETUP	distance target-array (cm)						
	23.5	18.5	15.5	13.5	11.5	8.5	
5ADC+5ATC+5MTC	8.8	11.0	12.4	13.2	14.1	14.6	ε_γ(%)
	39.0	39.6	39.7	39.8	39.9	39.5	P/T(%)
5ADC+5(ATC+MTC)	8.1	10.2	11.4	12.4	13.2	13.9	ε_γ(%)
	36.9	37.6	37.6	38.0	38.1	38.2	P/T(%)
5 ADC+10 ATC	11.0	13.5	15.1	16.1	16.9	17.1	ε_γ(%)
	40.0	40.5	40.7	41.1	41.2	40.8	P/T(%)
5 ADC+5 ATC	6.0	7.6	8.9	9.7	10.4	11.3	ε_γ(%)
	35.8	36.3	36.7	36.9	36.7	36.5	P/T(%)

2.2 Complementing 5 Double and 5 Triple AGATA Clusters with other MINIBALL configurations

Five additional MINIBALL configurations have been investigated with the AGATA configuration of Figure 1. Two of them included five MINIBALL detectors placed at 90 degrees and at target-detector distances of 170mm and 235mm. They are displayed in Figure 4.

The three other configurations included 4 MINIBALL clusters at 95 degrees plus 4 MINIBALL clusters at 129 degrees at the target-detector distances of (a) 206mm, (b) 250mm and (c) 400mm. They are displayed in Figure 5.

The efficiency and energy resolution results for all these configurations are displayed in Fig. 6 and Fig. 7, respectively. These results were obtained with a γ-ray energy of 1MeV, a v/c of 0.43, a target volume of 20×20×1 mm^3 but no target material. An Aluminium vacuum chamber was also included in the geometry and the reconstruct the Doppler corrected energy spectrum was performed with MGT tracking code. For sake of comparison, the results (without MINIBALL detectors) for the 5 ADC + 5 ATC configuration is also shown.

Numerical values of the previous representations are tabulated in the table of Fig. 8. Also given in red in the table is the efficiency when a Lead target 62×62×0.250 mm^3 is considered. The interation of the γ-ray within such a target is not negligeable when MINIBALL detectors are positioned near 90°.

Simple analytical calculations of the absolute Doppler broadening have been carried out

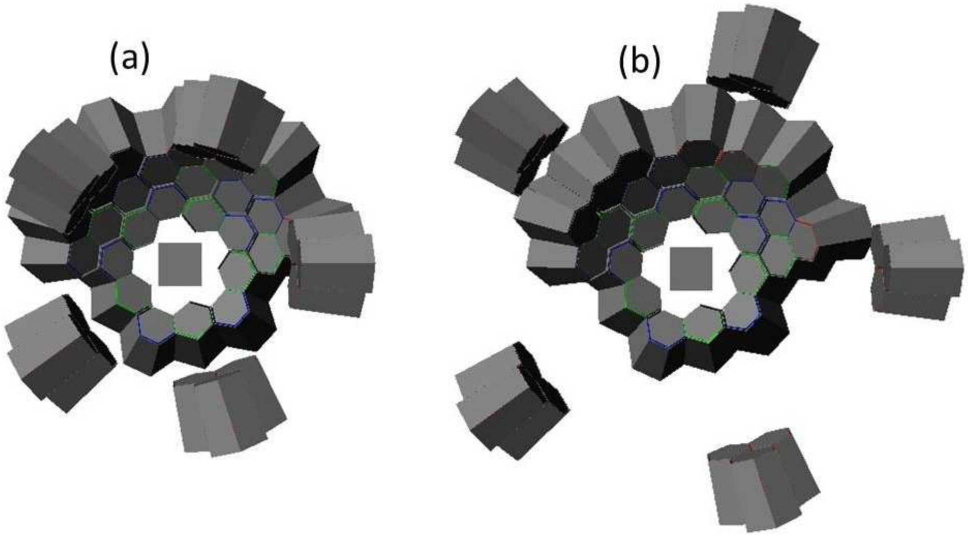

Figure 4: 5ADC+5ATC with 5MTC at 90 degrees and at 170mm (a) and 235mm (b) to the nominal target position)

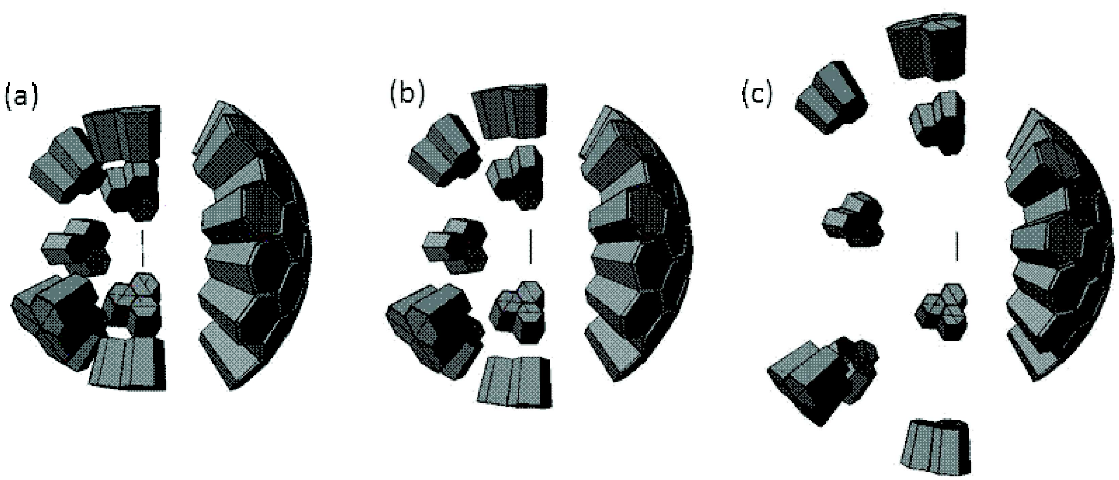

Figure 5: 5ADC+5ATC with 4MTC at 95° and 4MTC at 129°) positioned at 206mm (a), 250mm(b) 400mm(c) from nominal target position

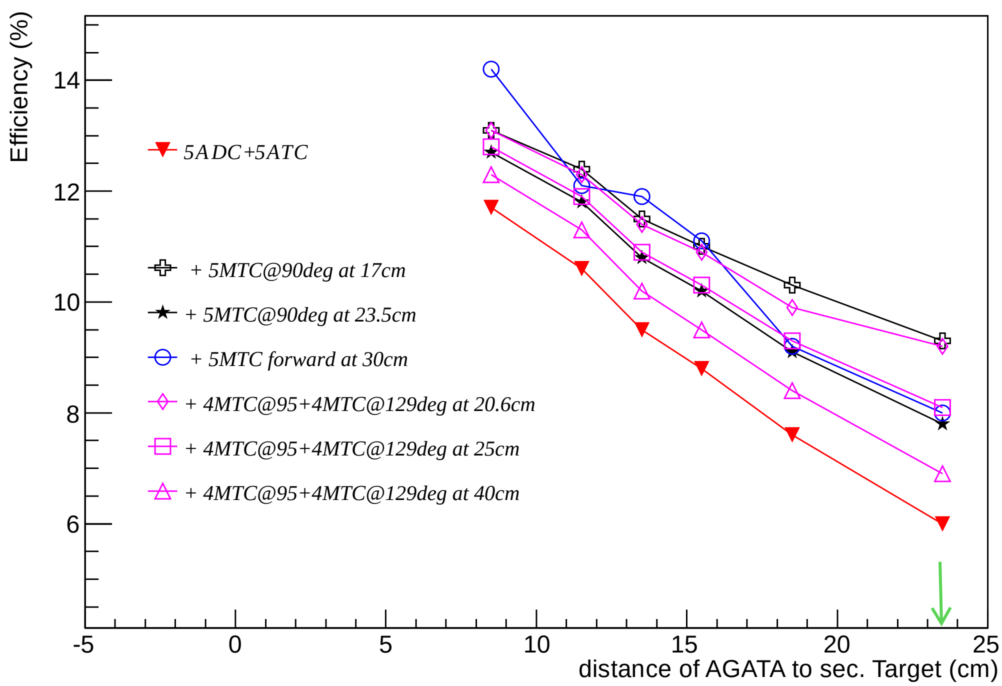

Figure 6: Efficiency for 5ATC+5ADC + diffirent MINBALL configurations. Simulations for β=0.43 and $E_{\gamma,\circ} = 1$ MeV. The green arrow corresponds to the nominal target position for AGATA.

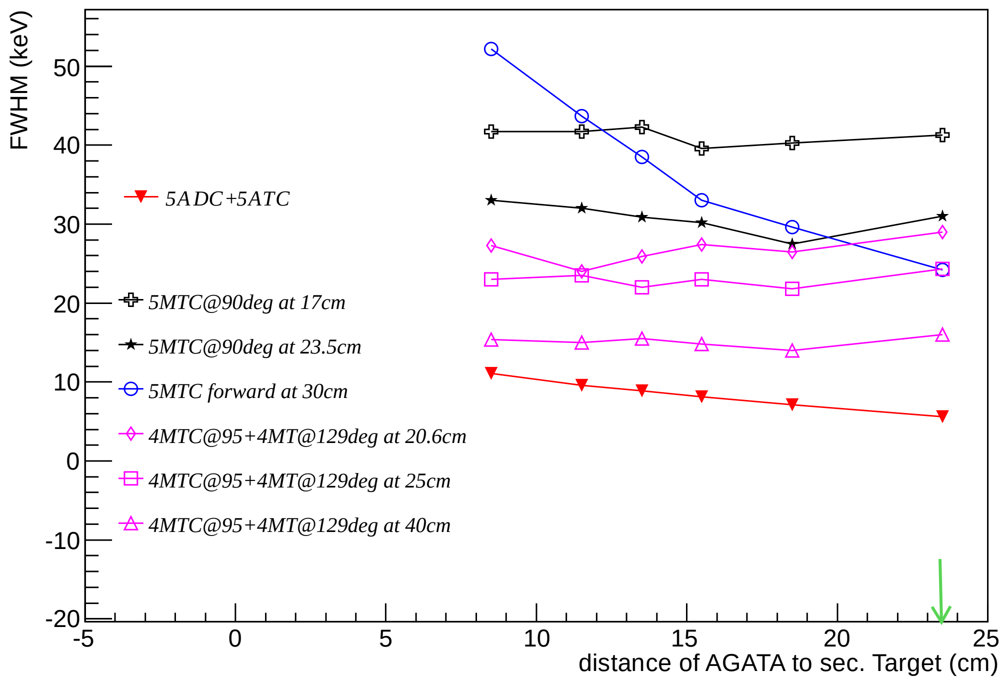

Figure 7: MINIBALL energy resolution for different configurations. The resolution with 5ATC+5ADC is also given for comparison. Simulations for $\beta = 0.43$ and $E_{\gamma,\circ} = 1$ MeV. The green arrow corresponds to the nominal target position for AGATA.

Without target material but with target volume (default volume=20x20x1):							
sourcetype4	distance Target-Array						
	23.5	18.5	15.5	13.5	11.5	8.5	
5ADC+5ATC	6 (5.9)	7.6	8.8	9.5	10.6	11.7	E(%)
235	5.6	7.1	8.1	8.9	9.6	11.1	FWHM (KeV)
with 5MTC90 @170mm	9.3 (8.8)	10.3	10.95	11.5	12.35	13.1	E(%)
	41.3	40.3	39.6	42.3	41.7	41.7	FWHM (KeV)
with 5MTC-90 @235mm	7.8 (7.5)	9.1	10.2	10.8	11.8	12.7	E(%)
	31.02	27.5	30.2	30.9	32	33	FWHM (KeV)
with 5MTC @ 300mm	8.0 (8.0)	9.2	11.1	11.9	12.1	14.2	E(%)
	24.2	29.6	33	38.5	43.71	52.2	FWHM (KeV)
with 4MTC-95 & 4MTC-129	8.1 (7.8)	9.3	10.3	10.9	11.9	12.8	E(%)
250mm	24.3	21.8	23	22	23.5	23	FWHM (KeV)
with 4MTC-95 & 4MTC-129	6.9 (6.7)	8.4	9.5	10.2	11.3	12.3	E(%)
400mm	16	14	14.8	15.5	15	15.4	FWHM (KeV)
with 4MTC-95 & 4MTC-129	9.2 (8.9)	9.9	10.9	11.4	12.3	13.1	E(%)
206mm	29	26.5	27.4	25.9	24	27.3	FWHM (KeV)
	() with Lead target 62.25 mm x62.25 mmm x 250 um						

Figure 8:

for MINIBALL and are given in Fig. 9. The calculations have been performed with the following parameters: $\Delta\theta = 12.5mm/235mm$; $beta = 0.43$; $\Delta\beta = 0.03$ and an intrinsic energy resolution of 0.2% at 1 MeV. If we assume that MINBALL clusters are at 90 degrees and that beta is constant (ie: we forget that the beam slows down in target) then the Doppler broadenning is dominated by the red curve which gives 23 keV FWHM. This is lower than the 31 keV predicted by the simulation for 5MTC at 90° and 235 mm away from the target as given in Fig. 7. A better agreement is obtained when taking $\Delta\theta = 17mm/235mm$.

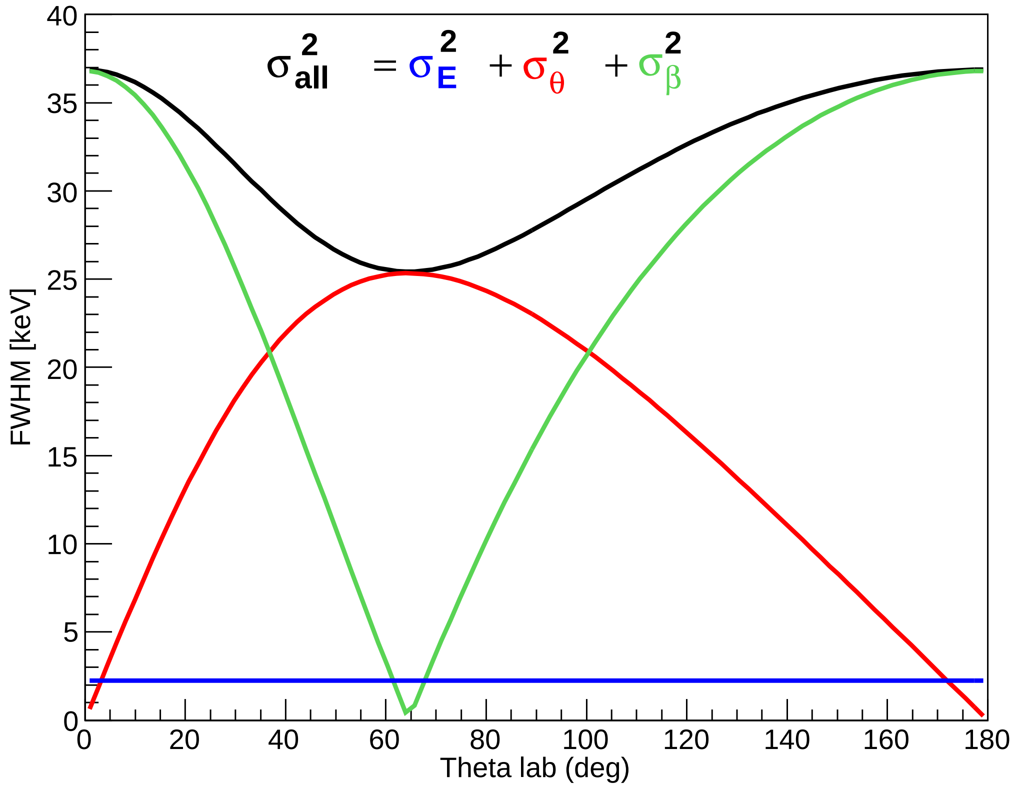

Figure 9: Doppler Broadening as function of the γ-ray polar angle and the different contributions

3 Resolution and lineshape effects: MINIBALL vs. AGATA

Resolution and lineshape effects in MINIBALL at 25 cm

The MINIBALL Configuration corresponds to 4 triple clusters at 95° and 4 triple clusters at 130°. The secondary target is always at the nominal position.

The γ-ray energy is reconstructed via the Doppler formula:

$$E_{\gamma,\circ} = E_\gamma \frac{1 - \beta cos\theta_\gamma}{\sqrt{1-\beta^2}} \tag{1}$$

where,

- E_γ is the measured γ-ray energy,
- β is the value of β **after** the target, i.e. what is measured with LYCCA.
- θ_γ is the angle at which the γ-ray was registered in the laboratory frame, assuming that it was emitted at the **center** of the target.

Figure 10 shows an analytical -simplified- calculation of the main contributions to the total energy broadening. The red curve ($\Delta\beta$) shows the contribution due to a velocity uncertainy of $\Delta\beta = 0.03$ at $\beta = 0.51$. However, this applies only for the case that the γ-transition happens inside the target volume. When the decay occurs after the target the velocity is well known (measured with LYCCA) and this contribution to the uncertainty practically vanishes (is affected only by the LYCCA ToF resolution). The blue curve ($\Delta\theta$) shows the contribution due to the uncertainty on the angle of the measured γ-ray, i.e. the spatial resolution of the detector. However, this assumes that the γ-decay happens in the center of the target. For long half-lives, the decays happen further downstream, which introduces an additional uncertainty on the reconstructed γ-ray energy. The latter effect is reflected in the MC-simulated spectra shown below for long half-lives.

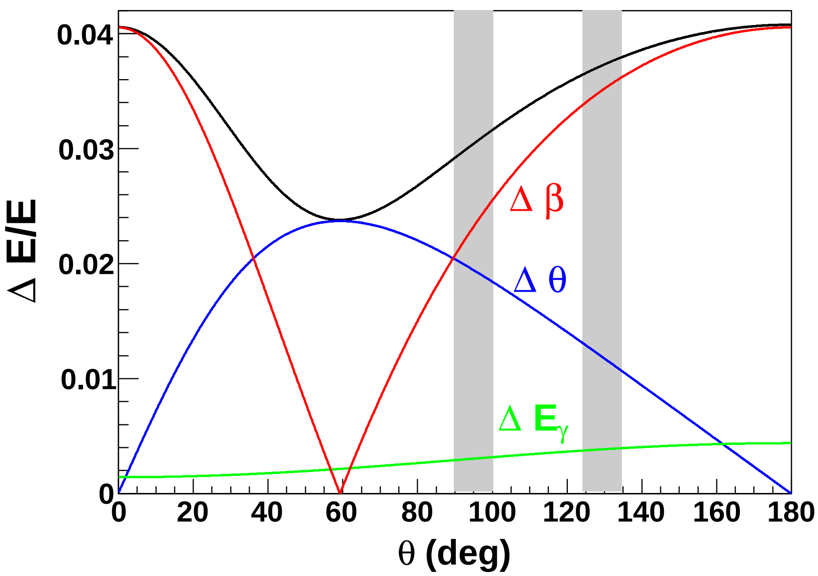

Figure 10: Contributions to the broadening of the reconstructed gamma-ray energy. Calculation made for the target at the nominal position, assumming a position uncertainty of ∼2 cm in MINIBALL (this determines $\Delta\theta$), for $E_{\gamma,\circ}$ = 1 MeV, β = 0.51 and $\Delta\beta$ = 0.03. The shaded regions show the main angles covered by the MINIBALL detectors in the 4 MTC@95°+4 MTC@130° at 25 cm.

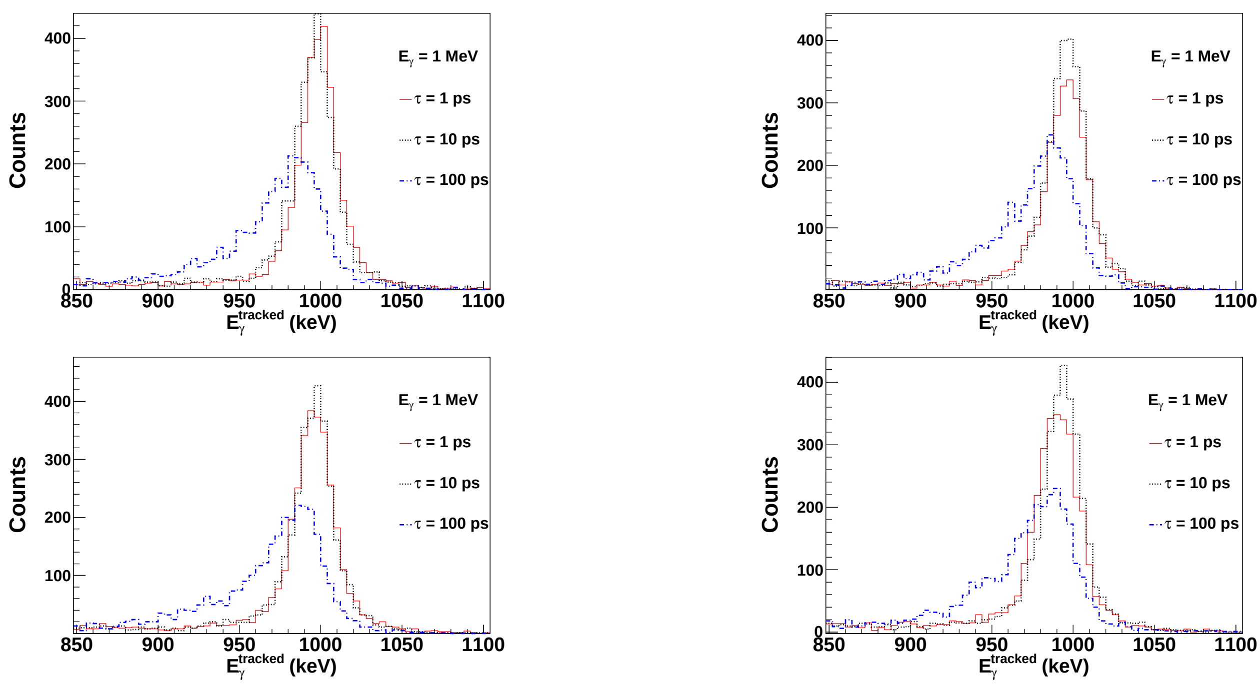

Figure 11: Miniball at 25 cm. Targets of Au 250 mg/cm^2 (top-left), Au 500 mg/cm^2 (top-right), Be 250 mg/cm^2 (bottom-left) and Be 500 mg/cm^2 (bottom-right). Spectra are shown with 4 keV/channel.

Table 2: MINIBALL with 4 clusters at 95° and 4 clusters at 130° at 25 cm from the target center.

	Target	τ (ps)			
material	thickness (mg/cm^2)	1	10	100	
Au	250	28	28	48	FWHM (keV)
		64	64	120	FWTM (keV)
Au	500	32	28	40	FWHM (keV)
		72	60	108	FWTM (keV)
Be	250	32	28	48	FWHM (keV)
		60	64	124	FWTM (keV)
Be	500	36	32	44	FWHM (keV)
		68	64	116	FWTM (keV)

Resolution and lineshape effects in MINIBALL at 40 cm

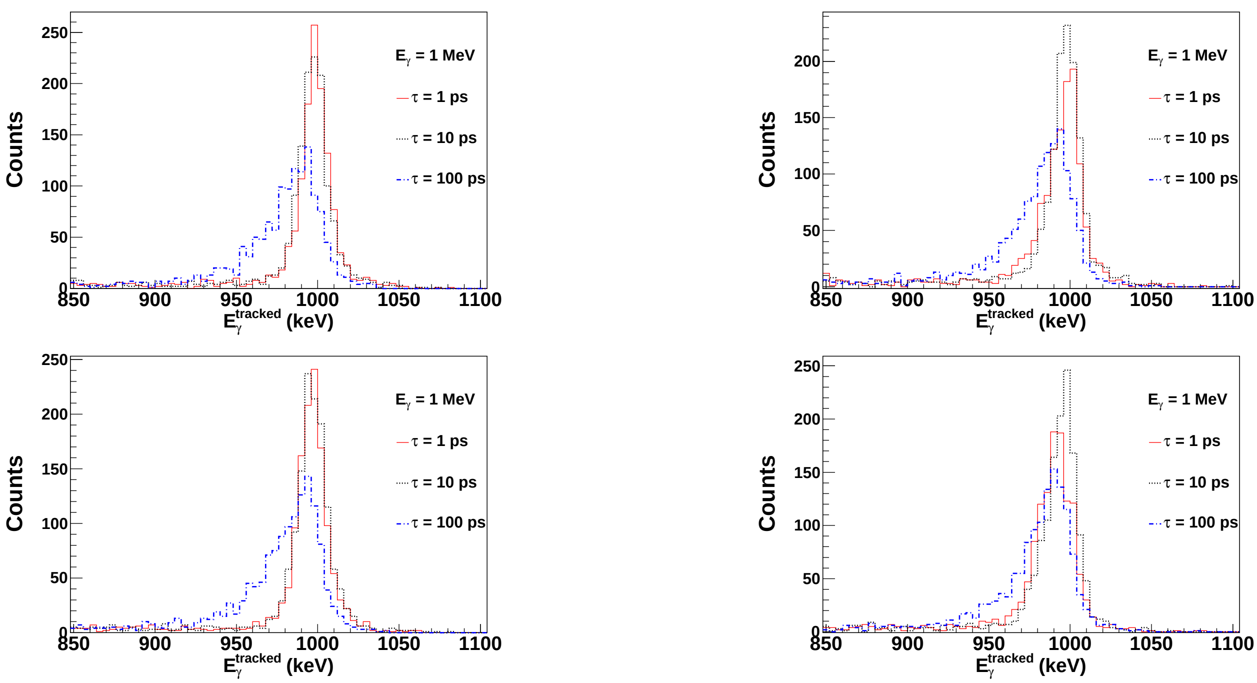

Figure 12: Miniball at 40 cm. Targets of Au 250 mg/cm^2 (top-left), Au 500 mg/cm^2 (top-right), Be 250 mg/cm^2 (bottom-left) and Be 500 mg/cm^2 (bottom-right). Spectra are shown with 4 keV/channel.

Table 3: MINIBALL with 4 clusters at 95° and 4 clusters at 130° at 40 cm from the target center.

	Target	τ (ps)			
material	thickness (mg/cm^2)	1	10	100	
Au	250	20	20	32	FWHM (keV)
		40	40	64	FWTM (keV)
Au	500	24	24	36	FWHM (keV)
		56	40	76	FWTM (keV)
Be	250	20	20	36	FWHM (keV)
		44	44	84	FWTM (keV)
Be	500	28	20	32	FWHM (keV)
		52	44	72	FWTM (keV)

Resolution and lineshape of 4 MTC at 95° and at 25 cm

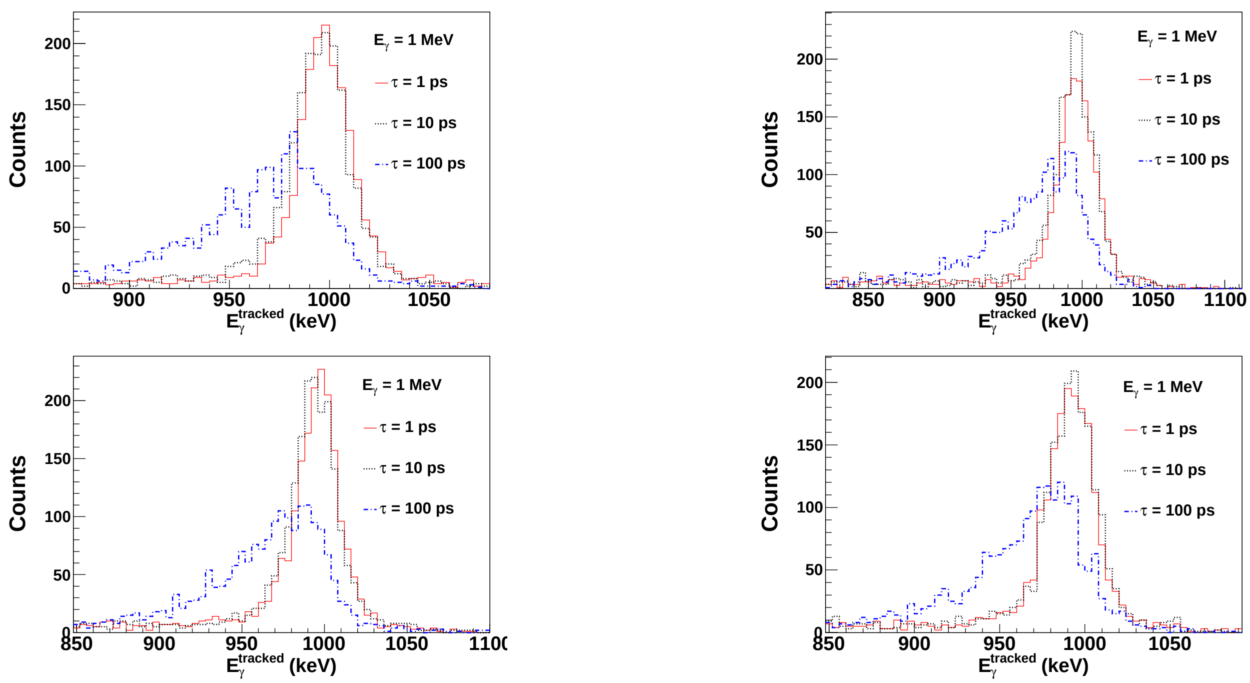

Figure 13: Only 4 Miniball at 95° and at 25 cm from target. Targets of Au 250 mg/cm^2 (top-left), Au 500 mg/cm^2 (top-right), Be 250 mg/cm^2 (bottom-left) and Be 500 mg/cm^2 (bottom-right). Rebinned to 4 keV/channel.

Table 4: MINIBALL with 4 clusters at 95° and at 25 cm from the target center.

	Target	τ (ps)			
material	thickness (mg/cm^2)	1	10	100	
Au	250	32	32	44	FWHM (keV)
		64	64	136	FWTM (keV)
Au	500	32	32	56	FWHM (keV)
		68	72	140	FWTM (keV)
Be	250	28	32	64	FWHM (keV)
		64	68	132	FWTM (keV)
Be	500	40	36	60	FWHM (keV)
		68	64	132	FWTM (keV)

Resolution and lineshape of 4 MTC at 130° and at 25 cm

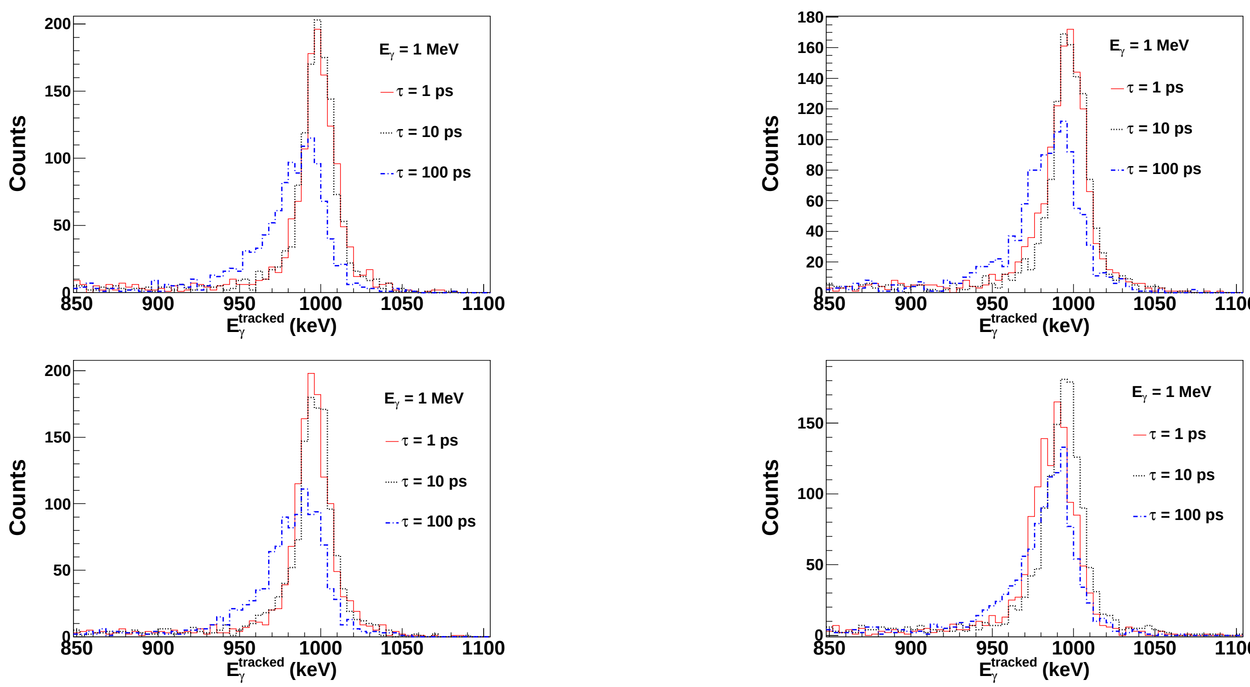

Figure 14: Only 4 Miniball at 130° and at 25 cm from target. Targets of Au 250 mg/cm^2 (top-left), Au 500 mg/cm^2 (top-right), Be 250 mg/cm^2 (bottom-left) and Be 500 mg/cm^2 (bottom-right). Spectra are shown with 4 keV/channel.

Note that, at least for transitions with a halflifes of more than ~1 ps, most decays happen already beyond the target. In these sitations the velocity of the reaction product measured with LYCCA coincides with the velocity of the fragment at de-excitation time, and therefore

Table 5: MINIBALL with 4 clusters at 130° and at 25 cm from the target center.

Target		τ (ps)			
material	thickness (mg/cm^2)	1	10	100	
Au	250	24	24	36	FWHM (keV)
		48	48	88	FWTM (keV)
Au	500	28	24	36	FWHM (keV)
		60	48	80	FWTM (keV)
Be	250	28	24	40	FWHM (keV)
		56	56	72	FWTM (keV)
Be	500	36	24	28	FWHM (keV)
		56	52	76	FWTM (keV)

the contribution to the uncertainty due to β (i.e. Δ_β) vanishes. Indeed, in most cases the uncertainty in the reconstructed γ-ray energy is dominated by the angular resolution (Δ_θ), which is maximum at about 60°, and degreases towards larger angles.

Resolution and lineshape in AGATA (5 ADC+5 ATC) for relative comparison vs. MINIBALL

The AGATA configuration corresponds to 5 ATC and 5 ADC. The target position is always the nominal.

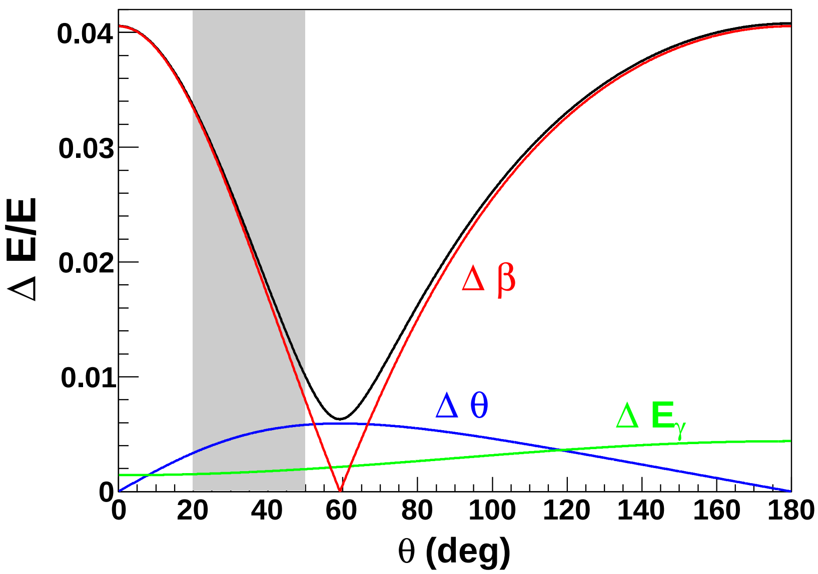

Figure 15: Contributions to the energy broadening of the detected gamma-ray. Calculation made for the target at the nominal position, assumming a position uncertainty of 5 mm in AGATA (this determines $\Delta\theta$), for $E_{\gamma,\circ}$ = 1 MeV, $\beta = 0.51$ and $\Delta\beta = 0.03$. The shaded region shows the angles covered by the 5 ADC + 5 ATC AGATA configuration with the target in the nominal position.

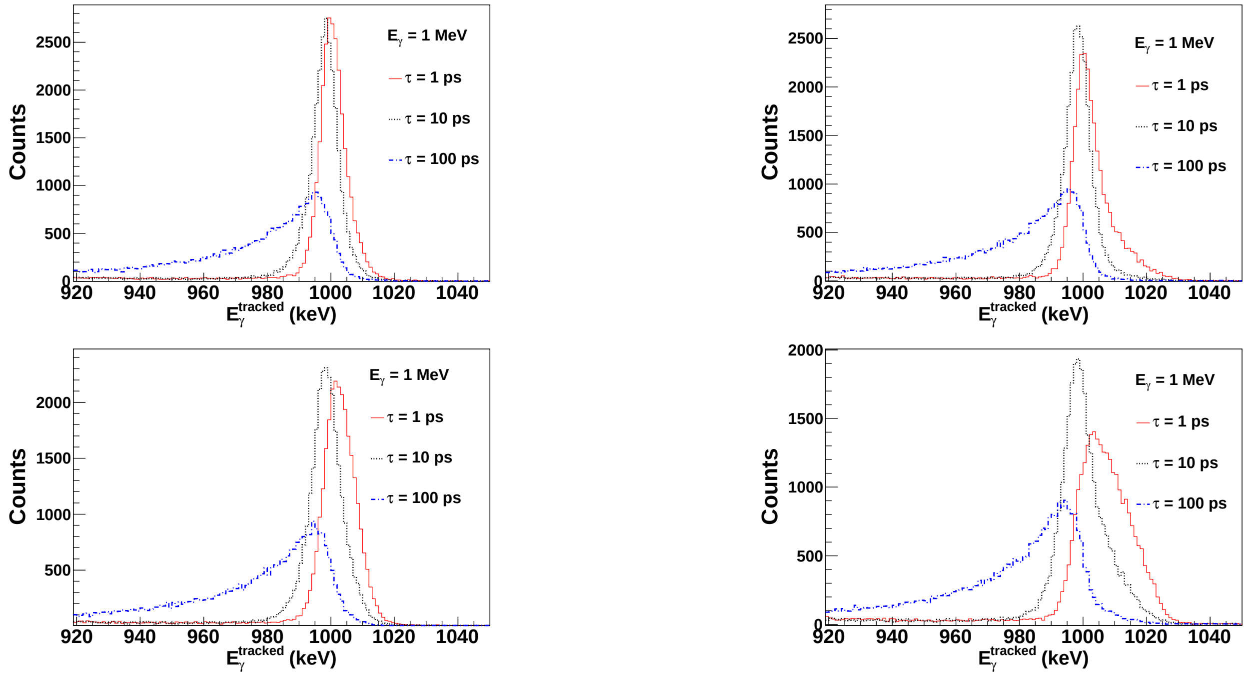

Figure 16: Targets of Au 250 mg/cm^2 (top-left), Au 500 mg/cm^2 (top-right), Be 250 mg/cm^2 (bottom-left) and Be 500 mg/cm^2 (bottom-right). Spectra are shown with 1 keV/channel.

Table 6: AGATA with 5 ADC and 5 ATC.

Target		τ (ps)			
material	thickness (mg/cm^2)	1	10	100	
Au	250	10	9	22	FWHM (keV)
		20	20	80	FWTM (keV)
Au	500	10	10	22	FWHM (keV)
		25	21	80	FWTM (keV)
Be	250	13	11	21	FWHM (keV)
		22	24	83	FWTM (keV)
Be	500	20	12	23	FWHM (keV)
		34	31	90	FWTM (keV)